

# Broadband femtosecond circular dichroism spectrometer with white-light polarization control

Anton Trifonov,<sup>1</sup> Ivan Buchvarov,<sup>2</sup> Andreas Lohr,<sup>3</sup> Frank Würthner,<sup>3</sup> and Torsten Fiebig<sup>1</sup>

<sup>1</sup>*Eugene F. Merkert Chemistry Center, Boston College, 2609 Beacon St., Chestnut Hill, Massachusetts 02467, USA*

<sup>2</sup>*Department of Physics, Sofia University, 5 James Bourchier Blvd., Sofia 1164, Bulgaria*

<sup>3</sup>*Institute of Organic Chemistry, Am Hubland, D-97074 Würzburg, Germany*

(Received 21 October 2009; accepted 6 February 2010; published online 15 April 2010)

A broadband, femtosecond transient circular dichroism (TRCD) spectrometer has been developed and tested in the wavelength range from 350 to 700 nm. The spectrometer uses a femtosecond probe white light with well-defined circular polarization. The latter is modulated by the polarization of a narrowband seed pulse. We have implemented a dual-beam probe geometry with phase-locked detection technique to increase the signal-to-noise ratio and to reduce optical artifacts. The spectrometer allows the acquisition of TRCD spectra with subpicosecond time resolution and typical noise levels of  $10^{-4}$  absorbance units. The performance of this instrument has been demonstrated on bis(merocyanine) nanorod aggregates in tetrahydrofuran/methylcyclohexane solution. The case study confirmed that this spectrometer is effective for the investigation of chiral properties in various molecular and nanostructural systems that have transient spectra in the UV-visible spectral range. © 2010 American Institute of Physics. [doi:10.1063/1.3340892]

## I. INTRODUCTION

Circular dichroism (CD) spectroscopy has been widely applied as a tool in material sciences, chemistry, biology, and physics.<sup>1</sup> Molecules that are optically active (chiral) exhibit CD, i.e., a difference in extinction for left and right circularly polarized light:  $\Delta\varepsilon = \varepsilon_L - \varepsilon_R$ . The CD effect originates from the fact that electric and magnetic transition dipole moments are not perpendicular to each other (which results in a helical net electron displacement during excitation). While chirality is necessary for observing a CD spectrum, the molecules (i.e., chromophores) do not have to be chiral to show a CD signal if they are spatially oriented to form a chiral array as typically found in biopolymers such as folded proteins or nucleic acids. The latter case is commonly described as exciton-coupled CD spectroscopy and has been advanced by Harada and Nakanishi.<sup>2,3</sup>

As far as CD is an absorptive property of a material quantified by the difference in the extinction coefficients for right and left circularly polarized light, there are two main approaches utilized to measure CD spectra. In *ellipsometric* CD measurements, the change in the ellipticity of a highly elliptically polarized light beam upon its passage through a circularly dichroic sample is detected. Any polarization state of light can be viewed as a superposition of circularly left and right polarization with certain amplitude and phase. Passing through dichroic (or birefringent) materials will induce changes in the relative amplitudes (and phase) of left and right circular polarization. Hence, the ellipticity of the input beam polarization is changed too. By measuring these changes for both left and right elliptically polarized probe (pr) beams, it is possible to determine both the sign and magnitude of the CD.<sup>1,4</sup> Although successfully applied in many nanosecond time-resolved CD measurements, the el-

lipsometric approach has inherent drawbacks.<sup>1,5</sup> Any circular and linear birefringence of the sample, sample cell, or optical elements in the beam path can generate artifacts which could be on the same order or even higher than the expected CD signal. The second approach (which is used in modern commercial steady-state CD spectrometers) is based on the *direct measurement of the differential absorption* of right and left circular polarized light, using polarization modulation and phase-locked detection techniques to increase the signal-to-noise. The principle of time-resolved CD (TRCD) spectroscopy is to measure CD spectra as a function of time after rapid initiation of the dynamics of interest. The existing methodology for subnanosecond time-resolved CD<sup>1,6</sup> is closely related to conventional pump-probe detection schemes where two ultrashort laser pulses (pump and probe) with a variable time delay between each other are used. The first pulse initiates a dynamical process (e.g., chemical reaction) by photoexciting a chromophore in the sample while the second pulse is probing the CD spectrum after the system has evolved in time. Before entering the sample the probing beam polarization is modulated using an acousto-optical or electro-optical modulator just like in a conventional CD spectrometer. The probing laser beam is generated by a tunable picosecond or femtosecond laser and the TRCD measurement is performed at fixed wavelength.<sup>1,6,7</sup> Therefore, obtaining the entire TRCD spectrum requires tuning of the wavelength of the pr laser beam over the whole spectral range of interest while the extremely small TRCD signals have to be detectable. Also, most CD spectra of molecules or molecular assemblies are quite complex and data from time-resolved measurements with single-wavelength detection<sup>1</sup> are difficult to interpret without obtaining the entire TRCD spectrum.

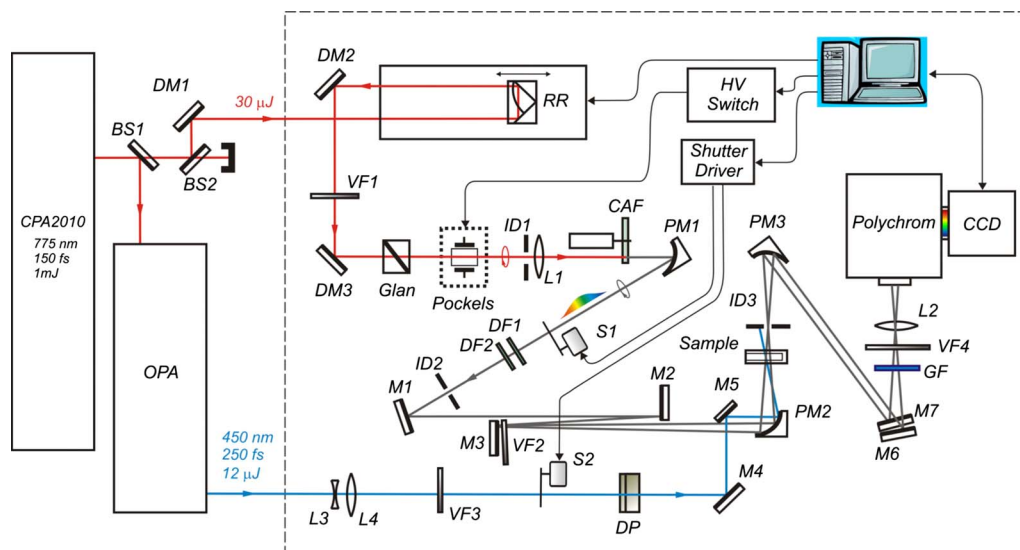


FIG. 1. (Color online) Schematic layout of the transient femtosecond TRCD spectrometer.

Here we present a new approach for broadband femtosecond TRCD spectroscopy, based on polarization-controlled femtosecond white-light (WL) generation. We demonstrate a sufficiently high degree of polarization control of the laser-generated WL over a wide spectral range from 350 to 700 nm simultaneously. The described spectrometer implements direct measurement of the differential absorption of right and left circular polarized light, using polarization modulation and phase-locked detection techniques to increase the signal-to-noise ratio. A monochromatic linearly polarized light beam from a femtosecond laser passes through an electro-optical modulator in which the polarization state of the beam is switched between right and left circular polarization. Furthermore, this modulated beam is used to seed a WL generator which preserves the polarization state of the incident beam. Subsequently, the generated probe light is directed through a sample and is processed by a synchronized detector (referenced at the modulation frequency). Hence, this technique eliminates the need for analyzing the polarization state of the beam after passing through the sample. As a result, the direct absorptive approach is less prone to polarization artifacts compared to the ellipsometric method.<sup>5,7</sup>

## II. EXPERIMENTAL SETUP: APPARATUS

The schematic diagram of the TRCD spectrometer is depicted in Fig. 1. The femtosecond pulses employed in the setup are produced by a commercial Ti:sapphire laser system CPA2010 (Clark-MXR) with average output power 1 W at 1 kHz repetition rate. The amplified spectral bandwidth is 7 nm full width at half maximum (FWHM) with a center wavelength of 775 nm. The pulse duration is 156 fs (FWHM), assuming Gaussian pulse shape.

Approximately one third of the output of the regenerative amplifier [beamsplitter BS1 ( $R=32\%$ )] is used to pump a home-built two stage visible noncollinear optical parametric amplifier (OPA, Fig. 1). The output of the OPA is a chirped broadband pulse, tunable between 440 and 720 nm

with pulse energies between 4 and 15  $\mu\text{J}$ , depending on the wavelength. The output spectra have a bandwidth between 10 and 25 nm FWHM, depending on the central wavelength. The output pulses from the OPA are not compressed. The pulse width of the used excitation wavelength of 450 nm is 250 fs FWHM, assuming Gaussian pulse shape.

The TRCD spectrometer has two optical ports, one for the excitation beam (from the OPA) and another one for the infrared pulses (at 775 nm), used for generating the circularly polarized WL for probing. A small fraction (30 mW) of the amplifier beam is reflected by the beamsplitter BS2 and supplied to the probe optical port of the spectrometer. The beam is reflected by the dielectric mirror DM1 to an optical delay line, comprised of a hollow gold-coated retroreflector (RR) and a precise 306-mm translation stage with submicron step resolution, controlled via RS232 serial interface. The BS2 and the steering mirror DM1 are used to align the optical delay line for minimal ( $<0.1$  mm) beam displacement for the entire (2 ns) range of translation. The beam, reflected by RR, is directed by the steering mirrors DM2 and DM3 to the polarization-controlled WL generator, comprised of a variable neutral-density filter VF1, calcite Glan-laser polarizer prism (9 mm aperture, extinction ratio  $<10^{-5}$  for 775 nm), DKDP Pockels cell, variable iris diaphragm ID1, lens L1 ( $f=100$  mm), calcium fluoride plate, and UV aluminum coated parabolic mirror PM1 with effective focal length 76 mm. The 5-mm-thick  $\text{CaF}_2$  disk is mounted directly on the spindle of a precise ball-bearing motor and is rotated with  $2 \times 10^3$  rpm in order to avoid optical damage. The left or right circular polarization state of the input beam is set by the  $\lambda/4$  voltage on the Pockels cell, which for the used DKDP cell is 3.6 kV for 775 nm. A stable WL generation is obtained by adjusting the beam power (using VF1) to 3.6 mW, around two times above the generation threshold.

The generated WL is collimated by the mirror PM1. The dielectric filters (DF1 and DF2, with customized multilayer coatings) are used for attenuation (1:100) of the fundamental (775 nm) and to smooth the probe spectrum. After it passes the filters, the WL is reflected by the broadband aluminum

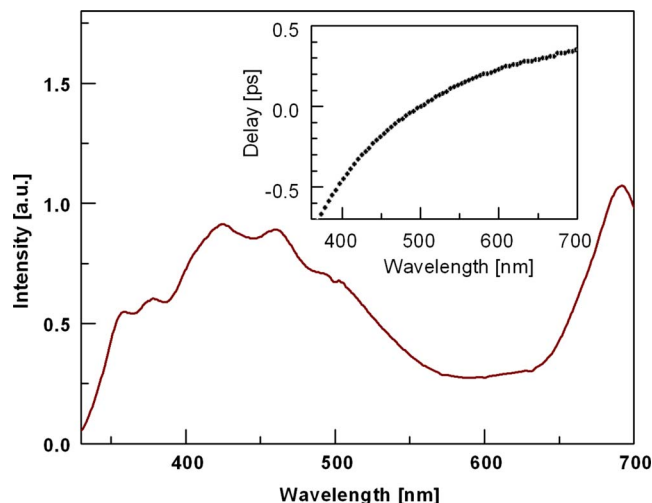


FIG. 2. (Color online) Typical spectral intensity of circularly polarized WL generated with seed at 775 nm, as detected by the CCD camera attached to the spectrometer. The inset shows the temporal chirp of the WL probing pulse.

mirrors M1 and M2 and is split into two beams, referred to as pr and reference (ref), using the reflective variable neutral-density filter VF2 and the aluminum mirror M3. The pr beam is reflected by the frontal metallic surface of VF2. The beam transmitted through VF2 is reflected by the aluminum mirror M4 and after a second pass through VF2, it is directed to the focusing mirror PM2 as a ref beam. The higher-order reflections from VF2 and M4 are blocked by beam stops. Adjusting the transmittance of VF2 enables the equalization of the intensities of the pr and ref at a level of around 25% from the incident WL. Both beams—between VF2 and the entrance slit of the monochromator—are shown in Fig. 1 as propagating in the plane of the figure, while in the optical setup they propagate exactly on top of each other. The pr and ref beams are focused into the sample by the UV aluminum coated parabolic mirror PM2 with an off-axis focal length of 100 mm. The distance between the focal spots on the sample cell is 2 mm. After passing the sample cell, the two beams are collimated by the parabolic mirror PM3 and directed, by the mirrors M5 and M6, through a variable neutral-density filter VF3. The focusing lens L2 ( $f=40$  mm) directs the beams to the entrance slit of an imaging polychromator (Jobin-Yvon Triax 180) equipped with 500-nm blazed, 150-l/mm diffraction grating. Both beams are independently detected and spectrally analyzed simultaneously as two spectral stripes on the surface of a  $1340 \times 100$ -element silicone charge coupled device (CCD) array (Princeton Instruments), cooled to  $-75$  °C. The CCD data are transferred via a USB 2.0 interface. The spectral resolution of the detection system is around 3 nm over the entire spectral range. The probe WL spectrum, recorded with the CCD camera is shown in Fig. 2. The usable spectral range is between 350 and 700 nm. The temporal chirp is characterized by the method described in Ref. 8 and it is found to span around 0.8 ps in the range between 360 and 700 nm (Fig. 2 inset).

The polarization state of the generated WL across the UV and visible range has been extensively examined in previous studies.<sup>9,10</sup> In order to prove the applicability of this

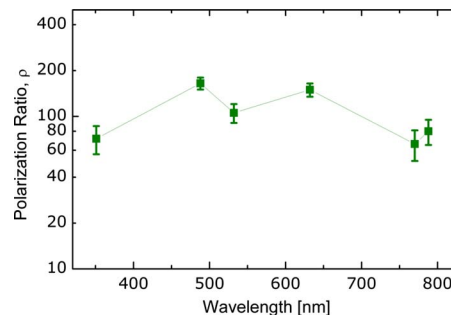


FIG. 3. (Color online) Polarization ratio of a WL generated with circular polarized input pulses. The points with error bars present the values when the circular polarization is analyzed using zero-order quarter wave plates at 351, 488, 532, 632, 760, and 790 nm. The line between points is used only for visual guidance.

method with the current setup, we made a brief investigation of the WL properties. First, the Pockels orientation and voltage (+3.6 kV) were carefully adjusted in order the transmitted laser pulses to have left-handed circular polarization. Second, the sample cell was replaced by a quarter wave retardation plate for a certain wavelength  $\lambda$  and a calcite Glan polarizer (analyzer). The preservation of the WL polarization at  $\lambda$  is given by the degree of which the quarter wave plate can reconvert the actual WL polarization to linear polarization which is examined further by the analyzer. Thus, the ratio  $\rho(\lambda) = I_{\text{par}}(\lambda) / I_{\text{perp}}(\lambda)$  of the intensities, transmitted through the analyzer at perpendicular  $I_{\text{perp}}(\lambda)$  and at parallel  $I_{\text{par}}(\lambda)$  orientation (with respect to the Glan), can serve as estimation how well the input circular polarization is retained in the process of WL generation. The data in Fig. 3 represent the measured values of  $\rho(\lambda)$  for six zero-order quarter wave plates at fixed wavelengths. The obtained  $\rho$  values for all different  $\lambda$  are above 70:1 and are close to the contrast ratios of the corresponding wave plates. These results show that the WL is very well circularly polarized (within  $\pm 1.4\%$ ) across the entire ultraviolet-visible (UV-VIS) spectrum (360–790 nm). The same experiment was repeated with negative quarter-wavelength voltage ( $-3.6$  kV) across the Pockels cell. It was found that the polarization ratio for the certain wavelengths does not depend on the handedness of the circularly polarized 775 nm pulses. Moreover, the intensity of the observed right-handed WL is practically identical (within  $\pm 1\%$ ) to the one of the left-handed WL. These results allowed us to conclude that the WL maintains the input circular polarization in great extent and it is fully suitable for TRCD measurement in the entire UV and visible spectral range.

In the TRCD arrangement of the setup (see Fig. 1), the excitation beam from the OPA is collimated using a beam expander, comprised of a pair of fused-silica lenses L3 and L4, with  $-50$  and  $+100$  mm focal length, respectively. The power of the excitation pulse is controlled by adjusting the variable neutral-density filter VF3. This scheme includes a Lyot calcite depolarizer (DP), suitable for scrambling the polarization of the excitation beam with spectral bandwidth of 16 nm (FWHM), in order to reduce the linear dichroism artifact.<sup>1</sup> Both the angle and the overlap between the excitation and the pr beam inside the sample cell are optimized by



tweaking the broadband silver mirrors M4 and M5. The focal spot size of the pump beam in the sample is optimized by finely tuning the distance between the lenses L3 and L4 and thus, adjusting the excitation beam divergence behind L4.

The CD at a given wavelength  $\lambda$  and the time delay  $\Delta t$  between the excitation and probe pulses is given by  $CD(\lambda, \Delta t) = A_L(\lambda, \Delta t) - A_R(\lambda, \Delta t)$ , where  $A_L$  and  $A_R$  are the absorbances of the sample for left-handed and right-handed circularly polarized light, respectively. Here, a negative time delay implies that the probe pulse arrives at the sample before the excitation pulse. In analogy to conventional pump-probe signals (see Ref. 8) in the current dual-beam geometry, the CD is measured as

$$CD(\lambda, \Delta t) = A_L(\lambda, \Delta t) - A_R(\lambda, \Delta t) \\ = \log_{10} \left[ \frac{I_L^{pr}(\lambda, \Delta t)}{I_L^{ref}(\lambda, \Delta t)} \right] - \log_{10} \left[ \frac{I_R^{pr}(\lambda, \Delta t)}{I_R^{ref}(\lambda, \Delta t)} \right]. \quad (1)$$

Here,  $I_L^{pr}$ ,  $I_R^{pr}$ ,  $I_L^{ref}$ , and  $I_R^{ref}$  denote the recorded pr and ref beam intensities on the corresponding spectral channel in the camera, respectively. The lower index characterizes the handedness of the polarization of the pr and ref beams: L: left-handed circularly polarized pulses; R: right-handed circularly polarized pulses. In the first observations of the spectra, collected using Eq. (1), we found that the amplitude of the spurious signal reaches several  $10^{-3}$  absorbance units (mOD), values comparable or even larger than the amplitude of the expected TRCD signal. This unwanted signal component originates mainly from the birefringence of the optical elements and the inherent polarization sensitivity of the diffraction grating in the polychromator.<sup>11</sup> Its amplitude does not depend on the sample excitation, hence it can be completely removed by subtracting a reference background signal, taken at negative delay  $\Delta t = t_N < 0$  from all the CD spectra, or  $TRCD(\lambda, \Delta t) = CD(\lambda, \Delta t) - CD(\lambda, t_N)$ . For practical purposes, the delay for reference measurement is selected  $t_N = -5$  ps. This subtraction eliminates the steady-state CD signal and the unwanted spurious contribution from the optics, producing only the transient CD component. After finishing a data acquisition cycle for a series of time delays, the averaged spectrum at  $t_N = -5$  ps, (containing steady-state CD and spurious signal) is subtracted from all the time-resolved spectra.

For the used CCD camera and the personal computer (PC) interface, the spectra acquisition rate is limited by the time of signal digitizing and transfer (12 ms). Thus, the optimal exposure time is in the range of 30–80 ms. The required millisecond regime for the Pockels cell voltage switching is satisfied by employing a customized high-voltage (HV) switch scheme [Fig. 4(a)], comprised of a precise regulated HV power supply (EMCO E101) and a computer-controlled bridge with two HV Reed relays (Meder Electronic HE12). Millisecond control of the exposure times is realized by implementing two optical shutters with fast miniature large-step motors and a custom-built motor driver, controlled through the parallel port of the PC. Synchronization between the computer-controlled shutters and the CCD camera is attained by triggering the CCD camera with a signal from the computer parallel port.

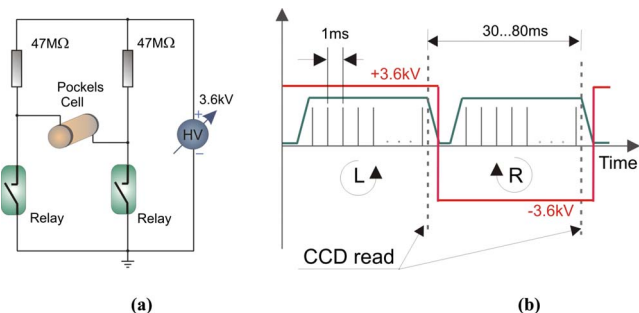


FIG. 4. (Color online) (a) HV switch schematic diagram and (b) timing diagram.

For a given delay between the excitation and the probe pulse, the optical signals are recorded in a sequence, illustrated in Fig. 4(b). First, the voltage over the Pockels cell is set to the positive quarter-wavelength voltage +3.6 kV. Thus, the generated probing WL is left-handed circularly polarized. The exposure time is controlled by the computer through opening and closing the shutters S1 and S2 simultaneously. In the current set of test measurements, the exposure time is set to 40 ms, allowing light from around 40 laser pulses to be accumulated on the CCD camera. Several milliseconds after the closing of the shutters S1 and S2, the two spectral stripes (pr and ref) on the camera are read out and the data are transferred to the computer memory, i.e., the spectral intensities  $I_L^{pr}(\lambda)$  and  $I_L^{ref}(\lambda)$  are recorded. Subsequently, the HV is switched to –3.6 kV, thus reversing the handedness of the generated probe light. Analogously, the exposure is repeated, allowing the corresponding spectra of  $I_R^{pr}(\lambda)$  and  $I_R^{ref}(\lambda)$  to be read and stored in the computer memory. Immediately after that,  $CD(\lambda)$  is calculated according to Eq. (1) and the result is stored in the computer memory. In order to reduce the shot-to-shot noise, several hundred (typically around 800) polarization change cycles are carried out and the measured  $CD(\lambda)$  signals are averaged.

### III. EXPERIMENT AND RESULTS

The sample used for the spectrometer evaluation is prepared with procedure described in details in Ref. 12. Briefly, approximately 460 mg (0.33 mmol) of bis(merocyanine) monomer (Fig. 5 inset) are dissolved in 2 mL tetrahydrofuran (THF) by stirring the solution for 1 h, followed by heating to 35 °C, and stirring for an additional 2 h. The concentration is  $1.66 \times 10^{-4}$  mol L<sup>-1</sup>. 300  $\mu$ L of this stock solution is mixed with 700  $\mu$ L of methylcyclohexane (MCH). The color of the solution changes from purple to yellow. The concentration is now  $5 \times 10^{-5}$  mol L<sup>-1</sup> in MCH/THF=70:30 vol %. The solution is kept for 24 h in room temperature to aggregate. The steady-state absorption and CD spectra (Fig. 5) are then measured with Jobin-Yvon and Aviv Model 202 spectrometers, respectively.

First, initial alignment of the spectrometer is performed. The optical delay line is aligned for minimal beam displacement for the entire range of translation using the mirror DM1 and the beamsplitter BS2. The Glan prism is set for maximum transmission of the horizontally polarized 775 nm beam. The HV is switched off. The transmission of the filter

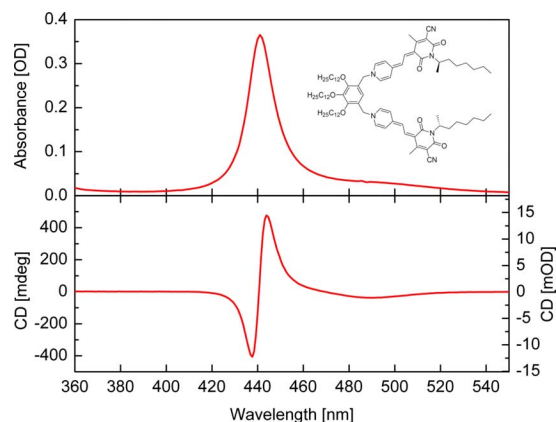


FIG. 5. (Color online) Steady-state absorption (upper panel) and CD spectra (lower panel) of merocyanine helical nanorods in solution, measured by commercial UV-VIS and CD spectrophotometers, respectively. The inset shows the chemical structure of the merocyanine dye monomer.

VF1, the diameter of the iris diaphragm ID1 and the position of the focusing lens L1 are tuned to obtain a stable, single-filament WL. The beam-splitting elements VF2 and M3 are adjusted in such a manner that (i) pr and ref beams have visibly identical intensities, (ii) both beams propagate exactly on top of each other, and (iii) the angle between the beams is around  $5^\circ$ . The mirror PM3 is aligned to collimate the transmitted trough the sample cell beams. The pair of mirrors M6 and M7 is carefully aligned so the probe and reference spectral stripes on the CCD camera are projected exactly on top of each other, with tolerance  $\pm 1$  pixel. The type of the color filter GF is selected for optimal equalization of the red and blue part of the probe spectrum. For this particular sample, the optimal type is Schott BG40.

The overlap of the excitation and pr beams in the sample is optimized, monitoring the excited state absorption signal from the merocyanine solution at positive time delay between the two pulses. For this purpose, the shutter opening sequence and the data calculation formula are set for direct absorption measurement, as described in Ref. 8.

After the coarse alignment is completed, a measurement on the excited state absorption dynamics of the merocyanine aggregates is performed. The DP is removed, allowing the sample to be excited with linearly (horizontally) polarized pulses. The HV on the Pockels cell is switched off; the Glan prism is set to  $54.7^\circ$  (“magic” angle) according to the optical table and the VF1 is reoptimized for stable WL generation. Several representative excited state absorption spectra are shown in Fig. 6. In the current sample the relaxation dynamics is best fitted with biexponential decay with time rates 20 and 700 ps (data not shown), allowing the spectral dynamics to be illustrated by several, nonchirp corrected spectra. However, if detailed observations in the time range between 0 and 1 ps are needed, it is possible the absorbance transients to be recorded with smaller temporal step and the signal to be corrected for temporal chirp using the procedure in Ref. 8.

As a final alignment step, the setup is finely tuned using a procedure, very similar to the one described in Ref. 13. The HV is set for positive quarter-wavelength for 775 nm (+3.6 kV). The Glan is set for maximal transmission and the

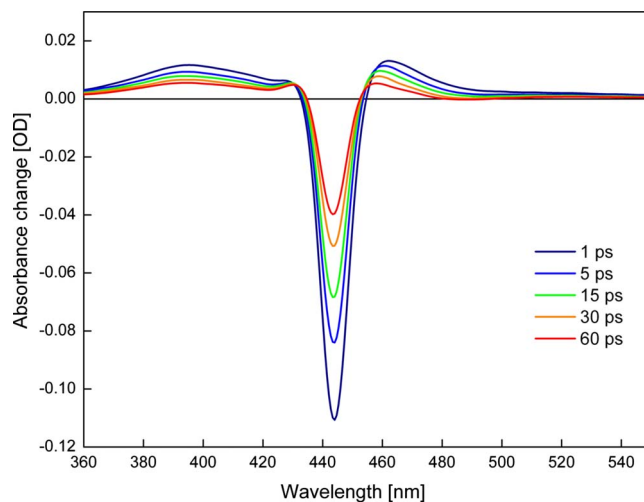


FIG. 6. (Color online) Excited state absorption spectra of merocyanine nanorod aggregates in MCH/THF solution. The corresponding time delays are shown in the legend.

VF1 is optimized for stable WL generation. The delay between excitation and probe pulses is set to +5 ps. The pan and tilt angles and the voltage of the Pockels cell are repeatedly adjusted, until the linear dichroism artifact (observed in real time) is minimized. After performing this step, the DP is returned to its initial place and the TRCD measurement is started. The TRCD spectra on several time delays are shown in Fig. 7.

#### IV. SUMMARY

A detailed description of a compact, all-solid state instrument for performing subpicosecond, broadband time-resolved transient CD spectroscopy is provided in this paper. The instrument is based on an amplified femtosecond Ti:sapphire laser system and produces broadband WL femtosecond pulses with circular polarization using a circularly polarized seed pulse. By employing this instrument, test TRCD measurements are performed and the results are in excellent

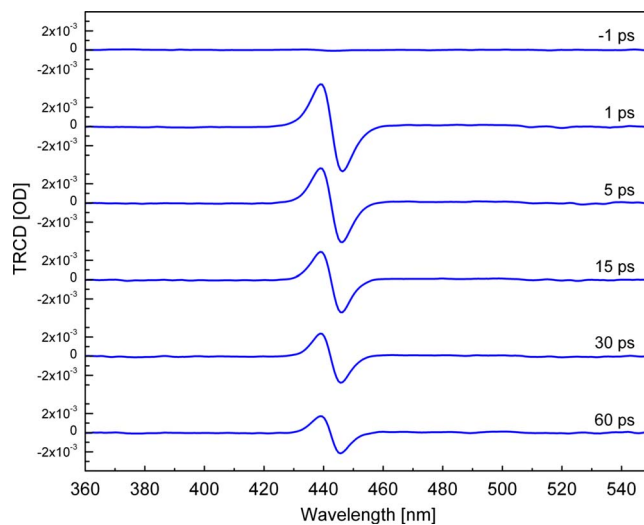


FIG. 7. (Color online) Time-resolved CD spectra at various time delays of merocyanine helical aggregates in MCH/THF.

agreement with those produced with a commercial steady-state spectrophotometer. This table-top instrument should therefore enable the core-level CD probing of ultrafast dynamics accompanying structural changes in a variety of molecular systems of great interest.

## ACKNOWLEDGMENTS

The authors would like to acknowledge the financial support for this project from the National Science Foundation under grant CHE-0521503 and from the Bulgarian Ministry of Science and Education under grant DRG 02/4.

<sup>1</sup>J. W. Lewis, R. A. Goldbeck, D. S. Kliger, X. L. Xie, R. C. Dunn, and J. D. Simon, *J. Phys. Chem.* **96**, 5243 (1992).

<sup>2</sup>N. Harada and K. Nakanishi, *Circular Dichroic Spectroscopy—Exciton Coupling in Organic Stereochemistry* (University Science Books, Mill Valley, 1983).

<sup>3</sup>D. A. Lightner and J. E. Gurst, *Organic Conformational Analysis and*

*Stereochemistry from Circular Dichroism* (Wiley-VCH, New York, 2000), pp. 423–456.

<sup>4</sup>C. Niezborala and F. Hache, *J. Opt. Soc. Am. B* **24**, 1012 (2007).

<sup>5</sup>S. C. Bjorling, R. A. Goldbeck, S. J. Milder, C. E. Randall, J. W. Lewis, and D. S. Kliger, *J. Phys. Chem.* **95**, 4685 (1991).

<sup>6</sup>X. L. Xie and J. D. Simon, *Rev. Sci. Instrum.* **60**, 2614 (1989).

<sup>7</sup>H. Mesnil, M. C. Schanne-Klein, F. Hache, M. Alexandre, G. Lemerrier, and C. Andraud, *Chem. Phys. Lett.* **338**, 269 (2001).

<sup>8</sup>M. Raytchev, E. Pandurski, I. Buchvarov, C. Modrakowski, and T. Fiebig, *J. Phys. Chem. A* **107**, 4592 (2003).

<sup>9</sup>A. A. Trifonov, I. C. Buchvarov, and T. Fiebig, in *Conference on Lasers and Electro-Optics/Quantum Electronics and Laser Science Conference and Photonic Applications Systems Technologies*, OSA Technical Digest Series (CD) (Optical Society of America, Washington, D.C., 2007), paper CM16.

<sup>10</sup>I. Buchvarov, A. Trifonov, and T. Fiebig, *Opt. Lett.* **32**, 1539 (2007).

<sup>11</sup>J. C. Cheng, L. A. Nafie, and P. J. Stephens, *J. Opt. Soc. Am.* **65**, 1031 (1975).

<sup>12</sup>A. Lohr, M. Lysetska, and F. Wurthner, *Angew. Chem., Int. Ed.* **44**, 5071 (2005).

<sup>13</sup>T. Dartigalongue and F. Hache, *J. Opt. Soc. Am. B* **20**, 1780 (2003).